

Crosstalk between Primase Subunits Can Act to Regulate Primer Synthesis in *trans*

Jacob E. Corn,¹ Paul J. Pease,¹ Greg L. Hura,² and James M. Berger^{1,*}

¹Department of Molecular and Cell Biology

²Lawrence Berkeley National Laboratory

University of California, Berkeley

Berkeley, California 94720

Summary

The coordination of primase function within the replisome is an essential but poorly understood feature of lagging strand synthesis. By using crystallography and small-angle X-ray scattering (SAXS), we show that functional elements of bacterial primase transition between two dominant conformations: an extended form that uncouples a regulatory domain from its associated RNA polymerase core and a compact state that sequesters the regulatory region from the site of primer synthesis. FRET studies and priming assays reveal that the regulatory domain of one primase subunit productively associates with nucleic acid that is bound to the polymerase domain of a second protomer in *trans*. This intersubunit interaction allows primase to select initiation sites on template DNA and implicates the regulatory domain as a “molecular brake” that restricts primer length. Our data suggest that the replisome may cooperatively use multiple primases and this conformational switch to control initiation frequency, processivity, and ultimately, Okazaki fragment synthesis.

Introduction

Cells rely upon the replisome, a large molecular machine that coordinates the action of dozens of discrete factors, to integrate chromosome unwinding with DNA synthesis. Because the entwined strands of DNA are antiparallel, the replisome must accommodate two distinct modes of operation. On the leading DNA strand, a DNA polymerase tracks in the same direction as a helicase to completely and continuously synthesize a daughter strand. On the lagging strand, the polymerase and helicase move in opposite directions. As a result, synthesis of the lagging strand stutters to produce discrete DNA segments of defined length, termed Okazaki fragments (Kornberg and Baker, 1992; Okazaki et al., 1968).

Because cellular DNA polymerases are incapable of *de novo* synthesis, the repeated initiation of lagging strand polymerization relies upon specialized RNA polymerases, termed primases, to provide short oligonucleotides for jump starting the replicative machinery. Though primases vary across different domains of life, bacteria rely upon a single subunit enzyme, DnaG, for primer synthesis. The activity of DnaG is tightly controlled in vivo to initiate short, regularly-spaced RNA primers from trinucleotide sites several thousand times per replication cycle (Kitani et al., 1985). Repetitive

primer synthesis thus defines a replication fork “clock” that dictates the formation of Okazaki fragments (Tougu and Mariani, 1996).

The DnaG protein is modular, consisting of three domains with distinct activities: an N-terminal zinc binding domain (ZBD), a central RNA polymerase domain (RPD), and a C-terminal replicase interaction domain. The function of the ZBD has remained elusive, although work with the distantly related DnaG-type primase-helicase of bacteriophage T7 (T7gp4) has suggested that it may play a variety of regulatory roles, including recognition of initiation sites and stabilization of nascent primers (Kato et al., 2003; Mendelman et al., 1994; Pan and Wigley, 2000). The RPD contains the catalytic site for primer synthesis (Keck et al., 2000; Podobnik et al., 2000), whereas the interaction domain binds the replicative helicase (DnaB) and tethers DnaG to the replication fork. Multiple primases can bind to a single helicase, but it is unclear how colocalization influences priming events (Bird et al., 2000; Mitkova et al., 2003; Valentine et al., 2001).

Despite extensive efforts, the mechanisms by which DnaG acts with the replisomal machinery to regulate lagging strand synthesis have remained elusive. For example, it is unclear why *E. coli* primase ignores ~97% of the trinucleotide recognition sites it encounters to only initiate an Okazaki fragment every 1.5–2 kb. Similarly, once primase has initiated synthesis, it is unknown how RNA polymerization is restricted to produce oligonucleotides that average 10–12 bases in length (Kitani et al., 1985). The means by which primase activity is blocked on single-stranded DNA substrates other than those found at the replication fork also remain unexplained.

To better understand primase function and help address these issues, we have carried out an extensive structure/function analysis of DnaG proteins from two bacterial species. Prior studies of phage T7 primase have shown that the ZBD and RPD within a subunit are uncoupled and suggested that the two domains associate in *cis* when a primer/template heteroduplex is present (Kato et al., 2003). In contrast, our crystal structures and SAXS analyses of fragments encompassing both the ZBD and RPD from *A. aeolicus* and *E. coli* show that bacterial primases preferentially adopt a compact conformation in which conserved residues on the ZBD are sequestered away from the active site of the associated RPD. Fluorescence resonance energy transfer (FRET) and additional SAXS experiments show that DnaG can transition from this state to a more extended form that disengages the two domains from one another. Unexpectedly, FRET and primase assays reveal that the ZBD of one primase can bind to primer/template associated with the RPD of a second molecule in *trans*. This interaction increases the catalytic activity of primase, enforces initiation specificity, and allows the ZBD to act as a molecular brake that restricts both processivity and primer length. When considered in the context of the replisome, our data support a model for primase function in which the ZBD regulates primer synthesis, and thus Okazaki fragment formation, by

*Correspondence: jmberger@calmail.berkeley.edu

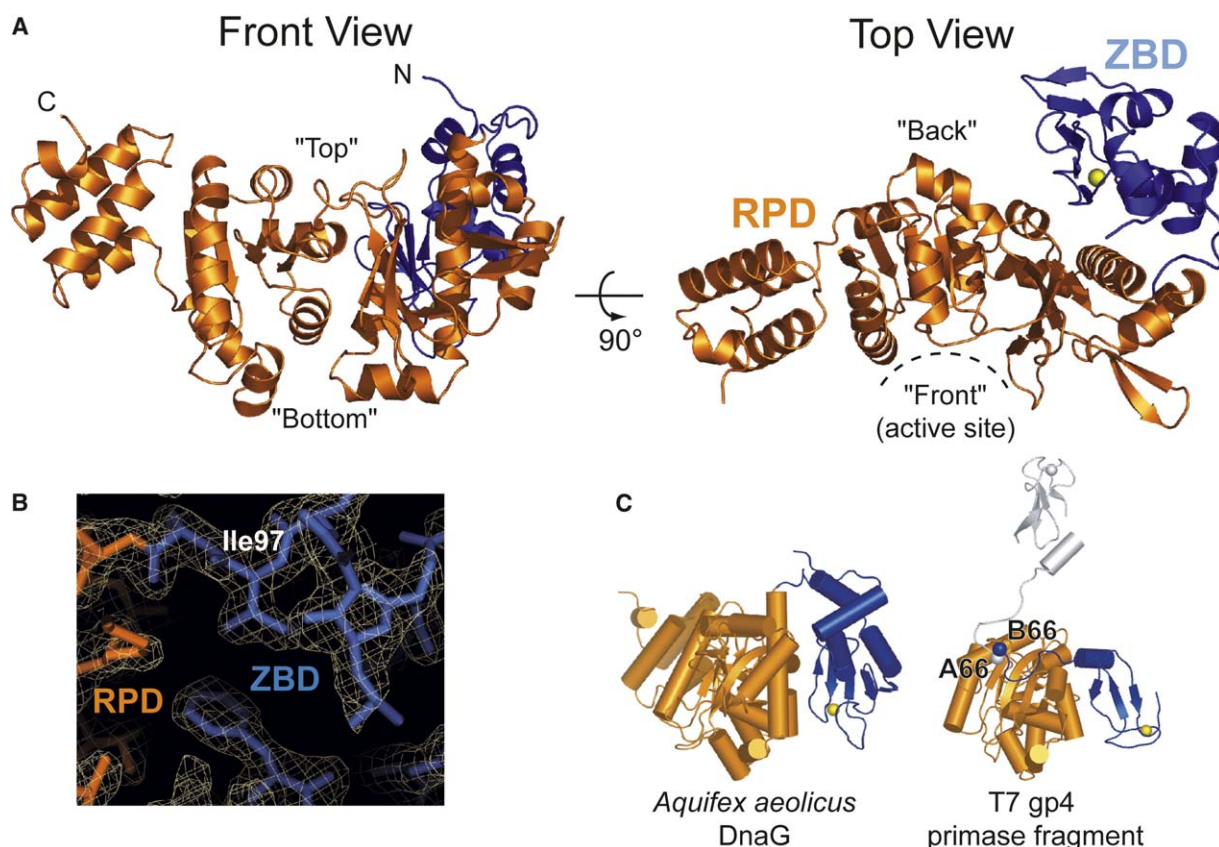


Figure 1. Crystal Structure of the *A. aeolicus* ZBD/RPD Primase Fragment

(A) The ZBD (blue) docks onto the back of the RPD (orange). The zinc ion is shown as a yellow sphere. All figures with molecular graphics were prepared by using PyMol (DeLano, 2002).

(B) $2mF_o - DF_c$ omit map of the linker between the *A. aeolicus* ZBD (marine) and RPD (orange) contoured at 1σ . Ile97 is labeled for reference. The omit map was calculated by using the 2.0 Å resolution native data set, with residues 88–102 removed.

(C) A domain-swapped packing configuration for the T7gp4 primase fragment (Kato et al., 2004) resembles that of *A. aeolicus* primase. The RPDs from both enzymes (chain A in T7gp4) are oriented similarly and colored orange. The ZBD from chain A of T7gp4 is colored white, whereas the ZBD from chain B is colored blue. The position of Tyr66 of T7gp4 is shown as a sphere in chains A (A66, white sphere) and B (B66, blue sphere).

facilitating crosstalk between an array of primases physically tethered to the helicase ring.

Results

Aquifex aeolicus Primase Forms a Compact Structure

To understand the interactions between the ZBD and RPD of bacterial primases, we determined the structure of a fragment (residues 1–407) that contains both regions from *A. aeolicus* DnaG to 2.0 Å resolution (Figure 1A). This ZBD/RPD fragment (*Aa*-ZBD/RPD) crystallized in three distinct crystal forms (see the Supplemental Data available with this article online). We first solved the *Aa*-ZBD/RPD structure from crystal form 1 by using a combination of multiwavelength anomalous dispersion phasing and molecular replacement (Supplemental Experimental Procedures). Crystal form 1 contains a single molecule per asymmetric unit, and continuous electron density is evident for all but the last four residues (Figure 1B). The final model was refined to an R_{work}/R_{free} of 20.5%/23.8% and shows excellent geometry (Table 1).

A recent structure of the DnaG-type primase fragment of T7 bacteriophage gene product 4 (T7gp4) captured this molecule in an extended state, such that the ZBD and RPD of a single protomer do not contact one another (Figure 1C; Kato et al., 2003). The structure of the *Aa*-ZBD/RPD differs significantly from this conformation, instead revealing a compact organization in which the ZBD and RPD associate closely. Several hydrophobic helices and one edge of the zinc ribbon from the ZBD dock into a cavity on the rear of the RPD's N-terminal subdomain and on the face opposite the catalytic center (Figure 1 and Figure S1). The conserved β sheet surface of the ZBD contacts the RPD, associating via several salt bridges and polar interactions, but is angled away by $\sim 45^\circ$ to form a narrow groove between the two domains. Surprisingly, the ZBD/RPD arrangement we observe is similar to the packing of these domains that occurs between protomers in crystals of T7gp4 (Figure 1C). Notably, the *Aa*-ZBD/RPD interface is preserved in all three crystal forms (Supplemental Data), suggesting that this docked configuration is a highly populated primase conformation.

Table 1. Data Collection and Refinement Statistics

	Form 1			Form 2	Form 3
Space group	P2 ₁ 2 ₁ 2 ₁			P2 ₁ 2 ₁ 2	1.13
Unit cell dimensions	43.2, 66.4, 138.1			138.0, 158.4, 43.9	141.4, 141.4, 81.4
Molecules per A.U.	1			2	1
Data Collection	Tm-λ1	Tm-λ2	Native	Native	Native
Wavelength (Å) ^a	1.4337	1.4013	0.9792	1.1150	1.1150
Resolution (Å) ^a	35–3.0 (3.11–3.0)	35–3.0 (3.11–3.0)	35–2.0 (2.07–2.0)	40–2.1 (2.19–2.1)	70–7.0 (7.39–7.0)
Reflections (measured/unique)	27,939/15,063	28,344/15,726	94,766/27,417	138,476/43,664	6790 (932)
Rsym (%) ^a	6.3 (20.6)	6.3 (20.7)	7.8 (28.6)	6.1 (39.6)	6.7 (18.2)
<I/σI> ^a	11.3 (2.5)	11.3 (2.7)	14.4 (3.4)	26.7 (5.1)	20.4 (8.3)
Completeness (%) ^a	95.0 (72.0)	95.8 (76.3)	99.0 (93.8)	92.4 (74.4)	97.1 (81.4)
Refinement	Form 1			Form 2	
R _{cryst} /R _{free}	20.5/23.8			21.2/25.6	
Average B factor (Å ²)	26.2			31.8	
Rmsd					
Bond lengths	0.014			0.013	
Bond angle	1.22			1.19	
Protein residues	403			786	
Water molecules	190			284	
Ramachandran (favored/allowed/generous/disallowed)	94.1/5.9/0.0/0.0			93.4/6.3/0.3/0.0	

^a Numbers in parentheses are for the highest resolution shell.

E. coli Primase Also Adopts a Compact Structure

Because bacterial priming has been best studied in *E. coli*, we pursued the remainder of our investigations by using DnaG from this organism as a model protein. Because crystals were not forthcoming, we employed SAXS, a solution-based approach for calculating low-resolution solvent envelopes and atomic distance distributions of particles, to determine whether the *E. coli* ZBD docks against the polymerase region. Data were collected from an *E. coli* primase construct encompassing both the ZBD and RPD (*Ec*-ZBD/RPD, residues 1–429) that was dialyzed into low-salt buffer (Experimental Procedures). The resulting distance distribution function was then used for ten independent rounds of domain reconstruction, using the crystal structure of the isolated *E. coli* RPD (PDB code 1DDE) as a starting point.

A consensus envelope (Figure 2A) generated from the most-populated volumes of the domain reconstructions was used to position a homology model of the *E. coli* ZBD based on the *B. stearothermophilus* structure (Pan and Wigley, 2000). The best fit of this model to the data places the C terminus of the ZBD near the N terminus of the RPD (Figure 2A). The distance distribution function and theoretical scattering curve calculated from this atomic model agree well with the experimental data and are a significantly better match than theoretical data calculated by using a compact “*Aquifex*-like” conformation (Figure 2B and Figure S2). Thus, although the *Ec*-ZBD/RPD conformation is distinct from that observed crystallographically for *A. aeolicus*, the ZBD still packs against the N-terminal subdomain of its associated catalytic core.

E. coli Primase Can Transition to an Extended State

To determine if the *E. coli* docked state is able to disengage and form an extended structure in a manner similar to T7gp4, we performed SAXS measurements of *Ec*-ZBD/RPD under increased ionic strength conditions.

Addition of 150 mM or 300 mM MgCl₂ to the SAXS buffer yielded particles with markedly larger radii of gyration compared to low-salt conditions (Figure 2B). This behavior correlated with a shift toward larger interatomic distances, suggesting that the ZBD can disengage from the RPD under conditions of increased ionic strength.

To confirm these results, we continued our examination of the association between the ZBD and RPD by using FRET. A suitable *Ec*-ZBD/RPD construct was made by mutating Thr348, which lies adjacent to the active site within the RPD, to cysteine. The ZBD of wild-type (wt) primase already contains several cysteines, most notably Cys39, that are available for labeling (Griep and Mesman, 1995). The Thr348Cys mutant is catalytically active and binds DNA templates as well as wt protein (Figure S3A, data not shown). We therefore used the labeled protein to directly examine the physical interaction between the ZBD and RPD as well as to determine how nucleic acids affect their interaction.

In low-salt conditions, similar to those used for the initial SAXS experiments, extremely strong FRET ($E = 0.806 \pm 0.0029$) was observed with a heterogeneously donor- and acceptor-labeled Thr348Cys mutant (Figure 3A). As a control, we denatured the labeled primase to determine the amount of background FRET arising from the labeling of Cys39 and two cysteines (Cys61 and Cys64) in the adjacent zinc-liganding motif (Figure S3B). High concentrations of either urea or guanidine HCl substantially decreased the FRET signal to the same efficiency (6 M urea, $E = 0.528 \pm 0.016$; 6 M GuHCl, $E = 0.525 \pm 0.026$), and doubly labeled wt protein, which contains reactive cysteines only within the ZBD, exhibited a very similar signal ($E = 0.480 \pm 0.005$) to denatured Thr348Cys (data not shown). Thus, even against a background in which FRET between dye molecules takes place within the ZBD ($E \approx 0.5$), substantial FRET can be observed between fluorophores localized to

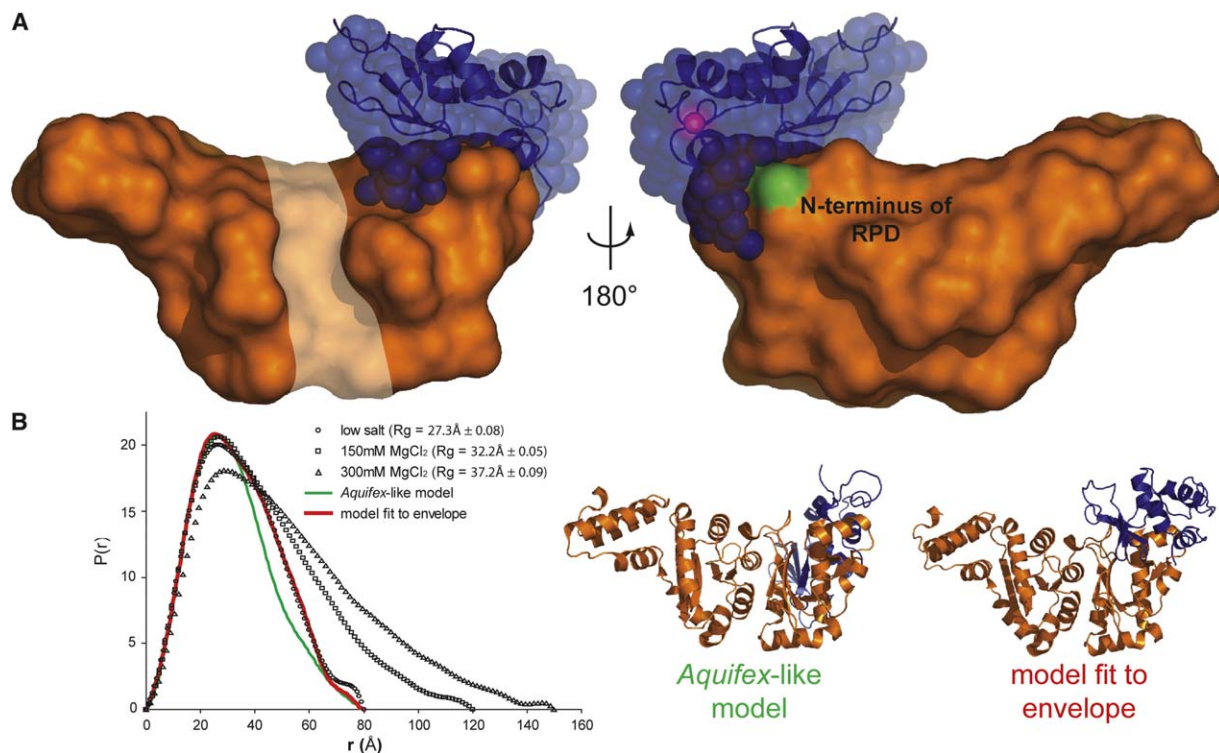


Figure 2. SAXS of the *E. coli* ZBD/RPD Primase Fragment

(A) Consensus envelope of the ZBD (blue spheres) obtained from domain reconstruction. The fitted homology model of the *E. coli* ZBD is shown as a ribbon diagram within the CREDO dummy-residue envelope. The putative path of primer/template through the active site is marked on the left panel by a white stripe (Keck et al., 2000; Podobnik et al., 2000). The C terminus of the ZBD and N terminus of the RPD are marked in magenta and green, respectively.

(B) Pair distance distribution functions of the *E. coli* ZBD/RPD in low-salt buffer (\circ) and buffer supplemented with 150 mM (\square) or 300 mM (\triangle) MgCl_2 . These experimentally determined curves are compared to the theoretical distance distributions of an atomic model of the ZBD/RPD fitted into the consensus envelope shown in (A) (red) and a conformation modeled on the *A. aeolicus* ZBD-docked crystal structure (green). The radius of gyration (Rg) determined from each experimental scattering curve is listed.

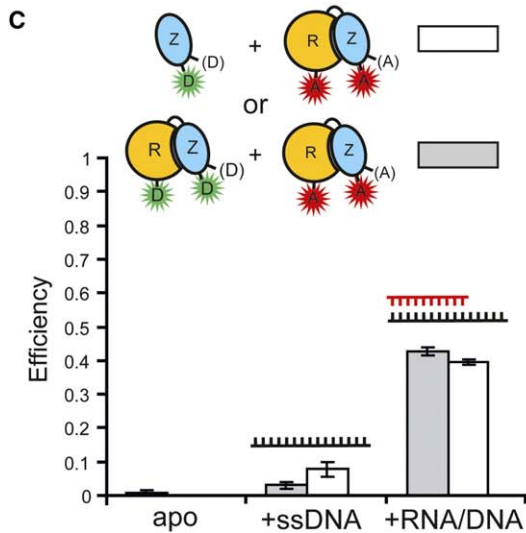
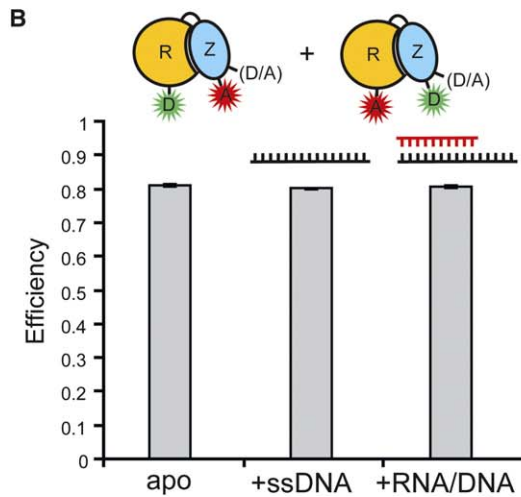
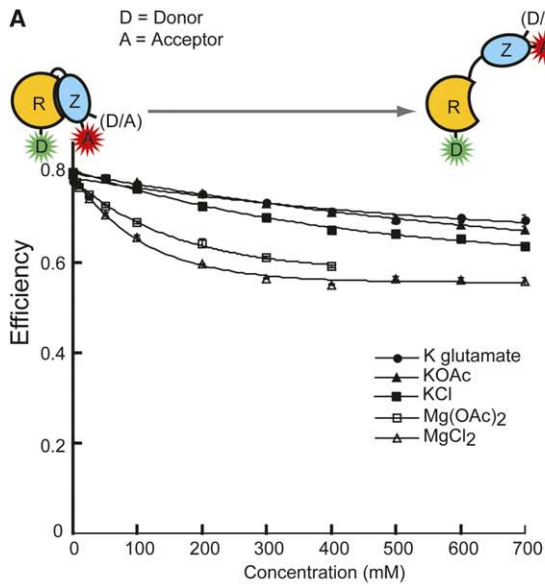
the ZBD and RPD ($E \approx 0.8$). As with our SAXS studies, this finding is consistent with the formation of a compact conformation in which the ZBD and RPD dock against each other.

To investigate the nature by which the ZBD associates with the RPD, we determined the FRET efficiency between these two domains in several different ionic conditions. Increasing concentrations of various salts significantly decreased FRET under conditions where *E. coli* primase is stable (e.g., 500 mM KCl) and in a manner that roughly follows the Hofmeister series ($\text{Cl}^- > \text{acetate} \approx \text{glutamate}; \text{Mg}^{2+} > \text{K}^+$) (Figure 3A). These data show that moderate ionic strength can increase the distance or alter the orientation between the ZBD and RPD. Together with our SAXS observations, this behavior suggests that the docked state of *E. coli* primase, like that of *A. aeolicus*, is stabilized by polar contacts and salt bridges. These studies further indicate that the RPD can release the docked ZBD, transitioning into an extended structure that likely exposes conserved residues on the surface of the ZBD. However, near 200 mM potassium glutamate, the concentration of these major intracellular osmolytes *in vivo* (Richey et al., 1987), FRET between the two domains is only partly diminished, implying that the docked state may predominate in the cell.

Primer/Template Binding by the *E. coli* Primase

To examine whether these conformational changes are associated with primer synthesis, we determined the extent to which nucleic acid substrates influence FRET efficiencies for the heterogeneously-labeled *Ec*-ZBD/RPD Thr348Cys construct. Upon addition of up to 100 μM of a single-stranded DNA template, FRET between the ZBD and RPD remained unchanged. The use of a short RNA/DNA heteroduplex with a 5' DNA overhang that mimics a primer/template substrate likewise did not affect FRET (Figure 3B).

Strikingly different behavior was observed in FRET assays using a mixed pool of an isolated, donor-labeled ZBD and an acceptor-labeled ZBD/RPD construct (Figure 3C). In the absence of nucleic acid ($E = 0.001 \pm 0.005$) or the presence of single-stranded DNA ($E = 0.077 \pm 0.022$), energy transfer was negligible. FRET became robust, however, in the presence of 100 μM of an RNA/DNA heteroduplex ($E = 0.396 \pm 0.008$). Thus, when presented with a specific substrate, a free ZBD is capable of associating with an RPD that is already covalently tethered to a different ZBD. Moreover, this response was maintained even when a donor-labeled ZBD/RPD construct was mixed with an acceptor-labeled ZBD/RPD construct (Figure 3C). Because one-half of any complexes forming *in trans* should comprise



nonproductive donor-donor- or acceptor-acceptor-labeled interactions, the greatest attainable FRET signal in this experiment can at most reach half maximum. Additionally, every ZBD/RPD molecule could, in principle, be capable of forming an intramolecular interaction between a ZBD and its covalently linked RPD bound to primer/template. Association in *cis* should therefore be more favorable than an interaction in *trans* and should furthermore preclude the formation of intermolecular complexes. Despite these obstacles, the presence of the primer/template nonetheless produced a FRET signal of ~0.5, indicative of a robust association between two primases in *trans*. Although these data do not preclude a *cis* interaction, they do demonstrate that the labeled ZBD and RPD of two separate protomers are readily capable of jointly binding to a primer/template substrate.

Regulation of Primer Synthesis by the ZBD

Although the T7 DnaG-type primase-helicase is incapable of RNA synthesis in the absence of the ZBD (Bernstein and Richardson, 1988), this appears not to be the case for bacterial primases (Keck et al., 2000). We therefore performed priming assays to delineate the mechanisms by which the ZBD regulates the function of bacterial primase. Studies using only the isolated *E. coli* catalytic domain showed that this region weakly synthesized primers whose lengths approached that of the template (Figure 4). This behavior occurred despite the presence of a 5'-CTG-3' initiation site lying 16 nt from the 3' end. Thus, it appears that the polymerase core alone cannot detect initiation sites and that it also preferentially extends or ligates all primers to their maximum templated length.

In contrast, the ZBD/RPD construct robustly synthesized a ladder of primers characteristic of normal primase activity (Figure 4B). These primers correctly initiated from the preferred template start site and remained centered around a distribution of 10–15 nt, a length similar to that found in vivo. This distribution was maintained even when the size of the template was increased to permit the synthesis of 24–32 mers. These data show that the ZBD not only increases activity

Figure 3. FRET Studies of Labeled ZBD/RPD Constructs

(A) Increasing salt concentration reduces FRET efficiency to baseline levels, consistent with undocking of the ZBD. Cysteines that ligand zinc within the ZBD may also be labeled (D/A) (Griep and Mesman, 1995), contributing to the high background. For heterogeneous-labeling experiments, the RPD and ZBD are equally likely to be labeled with either donor or acceptor; that is, every “D” shown is equally likely to be an “A” and vice versa.

(B) FRET efficiency of heterogeneously donor- and acceptor-labeled primase is not sensitive to binding single-stranded DNA or an RNA/DNA heteroduplex, suggesting that nucleic acid, unlike salt, either does not change the distance between the ZBD and RPD or does not undock the ZBD. As in (A), the identity of each fluorescent label is degenerate.

(C) Mixtures of homogeneously donor-only- or acceptor-only-labeled primase constructs display significant FRET but only in the presence of an RNA/DNA heteroduplex, indicating that the labeled primases can bind nucleic acid and that the ZBD of one molecule can contact the RPD of a second molecule and primer/template in *trans*. Mixtures of two ZBD/RPD pools are shown in gray. Mixtures of isolated ZBD and pure ZBD/RPD are shown in white. Error bars represent ± SD.

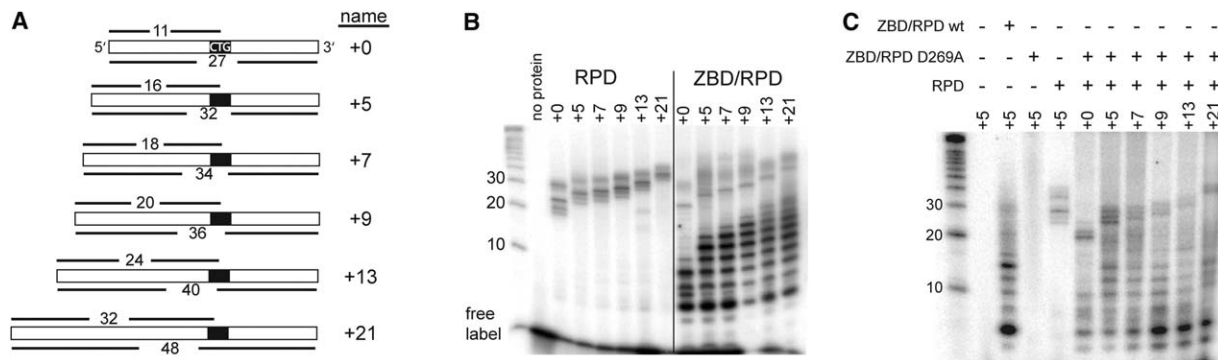


Figure 4. Regulation of Primer Initiation and Synthesis by *trans* ZBD/RPD Associations

(A) Schematic diagram of single-stranded oligonucleotides used in priming assays. An internal initiation site (5'-CTG-3') is marked by a black bar. The length of the entire oligonucleotide and the length from the starting "T" of the initiation site are also indicated. (B) The ZBD regulates RPD function. The RPD alone ignores an internal primer initiation site and synthesizes primers whose average length nearly matches that of the template. The ZBD/RPD synthesizes primers from the consensus CTG initiation site, greatly increasing specific activity, decreasing processivity, and restricting primer length to 8–15 nt. The gel is overexposed to highlight faint bands. Refer to (C) for a more representative view of the relative intensities of each band. (C) A catalytically dead ZBD/RPD construct containing a Asp269Ala mutation can complement a wt RPD to increase activity and restore synthesis of shortened primers.

and enforces initiation specificity, as has been observed for T7gp4, but that it also decreases processivity and restricts primer length.

To determine if *trans* interactions between the ZBD and RPD could regulate primer synthesis, we attempted to complement an isolated but catalytically active RPD with a ZBD/RPD construct containing an inactivating mutation in the catalytic center (Asp269Ala) (Godson et al., 2000). Because the Asp269Ala mutant binds nucleic acid normally (data not shown), a nonproductive *cis* interaction between its linked ZBD and RPD should be greatly favored over a *trans* interaction between monomers, particularly in the absence of the helicase. Notably, a mixture of the two differentially compromised primases exhibited an activity profile resembling that of the wt ZBD/RPD (Figure 4C). This effect was also observed when the isolated RPD was mixed with a ZBD/RPD construct containing a different inactivating mutation within the catalytic region (Asp347Ala, data not shown). The ZBD of one protomer is thus capable of disengaging from its covalently linked RPD to regulate primer synthesis occurring on a second protomer.

Discussion

Bacterial Primases Primarily Adopt a Compact State but Can Transition to an Extended Conformation

Recent work with the DnaG-type primase from T7 bacteriophage has shown that the ZBD and RPD of gp4 are uncoupled in the absence of primer/template (Kato et al., 2003). The crystal structure of *A. aeolicus* DnaG reveals a significantly different configuration, whereby the bacterial ZBD binds closely to the rear of its associated polymerase domain through a combination of hydrophobic and polar contacts. Domain reconstructions based on SAXS experiments using *E. coli* primase show that its ZBD also docks against the RPD, albeit through a different surface on the polymerase core than that seen for *A. aeolicus* (Figure 2). Despite this distinction, the conserved polar surface of the ZBD involved in the *A. aeolicus* docked state is also used for

the *E. coli* docked state, indicating that this association is surprisingly plastic.

This difference in ZBD/RPD packing is notable because variable protein-protein interfaces are part of an important emerging trend in biological systems that rely upon dissociable oligomeric contacts (Aloy et al., 2003; Brejc et al., 2001; Park et al., 2004). Consistent with the idea that the docked state is dynamic, our SAXS data show that the conformation of *E. coli* primase becomes extended at higher ionic strengths. Similarly, whereas strong FRET between dye molecules located on the RPD and ZBD further supports a dominant compact conformation, moderate ionic strength abolishes energy transfer, further suggesting that the conformational change observed via SAXS is due to an uncoupling of the two domains. Observations from other labs also provide support for this two-state transition. For example, limited trypsinolysis detects a salt-induced conformational change in *E. coli* primase upon addition of magnesium acetate (Urlacher and Griep, 1995). Cleavage occurs in regions of the ZBD that our structural studies show are relatively inaccessible when the ZBD and RPD are docked together (Figures 1 and 2 and Figure S1). Similarly, a cysteine within the bacteriophage T4 primase, which we would predict to be buried in the *A. aeolicus* ZBD/RPD interface, becomes accessible to chemical modification upon addition of single-stranded DNA, indicating that a docked resting conformation may exist in certain viruses as well (Valentine et al., 2001). Given that amino acids in the ZBD known to be important for primer synthesis are sequestered in the docked state (Kusakabe et al., 1999), these data suggest that primase may use this structural transition as a switch to control function, restricting the domain from participating in primer synthesis in one instance and freeing it to act in another.

The Primase ZBD and RPD Can Associate in *trans* to Regulate Primer Synthesis

Based on studies of T7gp4, it has been proposed that the ZBD of one primase molecule clamps down across

the catalytic face of its own RPD to bind primer/template and regulate priming in *cis* (Kato et al., 2003, 2004). Attempts to model a similar conformation for *Aquifex* primase proved unsuccessful, in part because the shortened linker between the ZBD and RPD, combined with additional α helices adjoining the zinc ribbon elements, occlude the putative exit path for primed DNA. Assuming that bacterial and phage primases both utilize an interaction between the ZBD and RPD to regulate catalysis, this analysis suggested that clamping between domains intramolecularly may be unfeasible for bacterial DnaG.

Instead, our biochemical studies indicate that an intermolecular *trans* association between the ZBD and RPD of two different primase molecules can regulate activity. For example, mixing of isolated donor-labeled ZBDs with acceptor-labeled ZBD/RPD proteins and primer/template yields robust FRET. Similar results are observed when individually donor- or acceptor-labeled pools of primase molecules containing both the ZBD and RPD are mixed in the presence of the RNA/DNA heteroduplex (Figure 3C). This intermolecular interaction occurs despite several factors that should favor intramolecular transactions. First, every RPD in the experiment is also covalently tethered to a ZBD, which should greatly favor association with a bound heteroduplex in *cis*, providing such an interaction is feasible. Second, the oligonucleotides used in the assay are in great excess (~2000-fold) relative to the protein, which should similarly favor *cis* interactions within a single protomer bound to primer/template. Despite these challenges, we observe relatively robust FRET between the ZBD and RPD of two separate molecules.

Given the extremely short length of the oligonucleotides used in this assay and the known dimensions of the ZBD and RPD (Keck et al., 2000; Pan and Wigley, 2000), it is highly unlikely that FRET can be attributed to two primases binding independently to the extreme ends of a single heteroduplex. Moreover, because no FRET is observed by using heterogeneously-labeled mixtures in the absence of nucleic acid or in the presence of single-stranded DNA, it appears likely that the ZBD of one primase molecule can assemble with the RPD of a second molecule only when specific target substrates are present. Although our experiments do not preclude a *cis* interaction between the ZBD and RPD, they indicate that a *trans* complex can form, even under conditions where intramolecular interactions should predominate.

Several possible functions for coupled interactions between primase subunits are suggested by the disparate activities of the RPD alone and a ZBD/RPD construct on templates containing a primer initiation site. Because the bacteriophage RPD is inactive in the absence of its ZBD (Kato et al., 2004), it has been assumed that the bacterial catalytic core is similarly inactive. Instead, we find that the isolated bacterial RPD retains a modest amount of activity and that this domain is surprisingly processive and synthesizes primers almost as long as the entire template (Figure 4B). When the ZBD is present, the bacterial primase becomes much more active and strongly prefers to initiate from the recognition sequence present within the template. The ZBD/RPD construct is also far less processive than the catalytic domain alone, generating a clear ladder of short primers

centered around 10–15 bases, which approximates the length of primers found in vivo (Figure 4B). The ZBD thus appears to act as a molecular brake that restricts the maximum length of primers synthesized by the RPD to fewer than 20 nt, even when presented with templates that have as many as 32 bases between the initiation site and the 5' terminus. Significantly, a ZBD tethered to an inactive RPD complements an active, isolated catalytic domain, producing short primers characteristic of the wt ZBD/RPD construct (Figure 4C). This finding shows that the ZBD from one molecule is capable of intermolecularly regulating primer synthesis occurring on a second primase protomer.

A Model for the Regulation of the Replication Fork Clock

Although our experiments do not directly address intermolecular primase interactions in the context of the replisome, previous studies in both bacteriophage and bacteria supplement our work and suggest that a *trans* complex between multiple primase molecules may constitute the active priming unit within the cell. Although primase is a monomer in the absence of substrate, several reports have hinted that multiple primases cooperate to regulate lagging strand synthesis. Primase binds nucleic acid as a multimer in both bacteria and some viruses (Khopde et al., 2002; Norcum et al., 2005). As many as three primase molecules bind to the helicase during lagging strand replication in bacteria, and up to six are present in T7 and T4 bacteriophage (Bird et al., 2000; Valentine et al., 2001). For *E. coli*, the primase:helicase ratio directly modulates function, with two to three primases per helicase producing maximal levels of activity (Johnson et al., 2000; Mitkova et al., 2003). Additionally, primer length distribution is altered in the presence of a helicase- and ATPase-deficient DnaB mutant under conditions reported to affect the symmetry of the helicase (Shrimankar et al., 1992; Yang et al., 2002), hinting that the spatial relationship between primase subunits may be important for function. Finally, neighboring primases functionally complement each other in both the T7gp4 and T4gp61 helicase-coupled priming systems to support primer initiation and hand off to the DNA polymerase (Lee and Richardson, 2002; Yang et al., 2005). These findings suggest that the intermolecular interaction between primase domains we observe could be recapitulated in the context of the helicase and may provide a general mechanism for controlling primer synthesis in both bacterial and phage-encoded DnaG-type priming systems.

If extended to the replisome, ours and others' data suggest that priming may be regulated within the cell by the propensity to form an intermolecular ternary complex between two primase subunits and the growing primer/template (Figure 5). This model envisions DnaB as a mobile DNA unwinding platform that serves three major functions with respect to lagging strand priming: producing single-stranded DNA for use as a template, increasing the local concentration of template and primase, and dictating the spatial arrangement of primases necessary to regulate priming. By analogy with T7gp4 (Toth et al., 2003), we hypothesize that multiple primases are arrayed on the amino-terminal surface of the bacterial helicase through their peg-like interaction

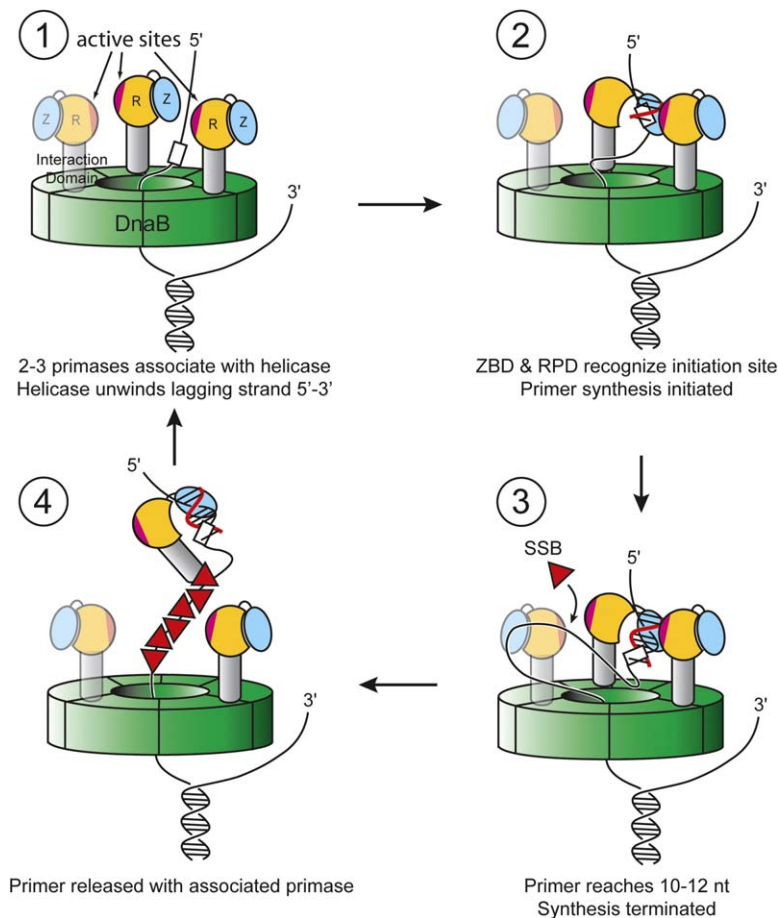


Figure 5. Model for Primer Synthesis at the Replication Fork

The replicative helicase (DnaB) serves as a “priming platform” to colocalize factors for initiating and regulating lagging strand synthesis. (1) As single-stranded DNA is released from the helicase, the ZBD of one primase can undock from its RPD and, working with the RPD of a neighboring subunit, scan for a preferred initiation site (white box). (2) Once engaged, the ZBD works with the RPD in *trans* to initiate primer synthesis. (3) As the nascent primer grows, interactions between the ZBD, RPD, and nucleic acid curtail synthesis to yield relatively short primers (10–12 nt in *E. coli*). Because DNA unwinding still occurs, the cessation of primer elongation may allow ssDNA to become exposed between the helicase and primase, an event that could serve to recruit SSB (red triangles) to the complex. (4) SSB, which can form a stable complex with DnaG and primer/template (Yuzhakov et al., 1999), may help disengage the assembly from the helicase by competing with DnaB for the interaction domain of DnaG.

domains (Oakley et al., 2005; Syson et al., 2005) and are positioned to accept newly unwound single-stranded DNA directly from the central hole of the ring. Our crystallographic, FRET, and SAXS data indicate that the ZBD of any given primase normally would remain docked in an inactive conformation against its own polymerase core in *cis*. However, an equilibrium with the extended state under physiological salt concentrations would permit the ZBD to disengage and scan for a primer initiation site and a neighboring RPD in *trans*. This conformational change may be the rate-limiting step to primer synthesis, which is known to occur at or before the formation of the first dinucleotide (Swart and Griep, 1995), and probably underlies the ability of the ZBD to activate of the catalytic core. After initiation, our priming assays indicate that the ZBD would restrict primer elongation occurring on the neighboring RPD to a defined length (~10–12 nt in *E. coli*). Once primer synthesis has terminated, there is evidence that a single primase molecule may be released from the helicase while remaining associated with the primer in an SSB-dependent manner (Yuzhakov et al., 1999). Analogy with T7gp4 suggests that these primase-primer interactions may be mediated by the ZBD (Kato et al., 2004).

This model, although speculative, reconciles disparate unexplained observations regarding the control of primer synthesis within the replisome. For example, the probability of encountering any trinucleotide primase recognition sequence is over ten times greater

than the actual frequency of Okazaki fragment initiation. In addition, the presence of various factors, including SSB, DnaB, and pol III, has been shown to induce primase to synthesize shorter oligonucleotides (Mitkova et al., 2003; Zechner et al., 1992). This restricted range of primer lengths may be critical for normal replication, because the coupled 5'–3' exonuclease and synthesis activities of pol I cannot efficiently replace more than ~10 nt at a time (Lewin, 1987). Thus, by the model proposed here, replisomal factors would not regulate primer synthesis by specifically controlling the activity of primase per se. Instead, they would act as nucleation centers to facilitate intermolecular associations between primase subunits. The frequency of initiation would be coupled to the concentration of primase in the cell and the probability that two to three protomers are associated with the replicative helicase at any given moment (Wu et al., 1992); once appropriately colocalized, cooperation between adjacent primase molecules would be sufficient to modulate primer initiation and length, thereby controlling Okazaki fragment synthesis and setting the replication fork clock. Because primase cannot efficiently function as a monomer, this mechanism would also provide a means to prevent unwanted priming at nonreplicative sites in the cell. Future studies to further address this model in the context of the replisome will highlight how interactions between primases and the rest of the replisome synergize to regulate lagging strand replication.

Experimental Procedures

Constructs, Expression, and Purification

The Aa-ZBD/RPD (residues 1–405), Ec-ZBD/RPD (residues 1–429), and Ec-ZBD (residues 1–102) were cloned into pET28b (Novagen) derivatives with a tobacco etch virus (TEV) protease-cleavable N-terminal hexahistidine tag. The *E. coli* RPD (residues 111–429) was cloned into pSV272, which generates a TEV-cleavable hexahistidine-tagged maltose binding protein fusion. All proteins were expressed in BL21 codon⁺ cells and purified by passage over a Poros MC-nickel column (Applied Biosystems), after which His₆-tags were removed with TEV protease. Proteins were then repassaged over the Poros MC-nickel column and run over a Sepharose S-200 gel filtration column (Amersham Biosciences) in 500 mM NaCl, 20 mM HEPES (pH 7.5), 10% glycerol, and 1 mM 2-mercaptoethanol.

The *A. aeolicus* DnaG-ZBD/RPD Structure

Initial screens produced three crystal forms (forms 1–3, [Supplemental Data](#)) from microbatch experiments. Form 1 crystallized out of 18%–22% EtOH, 55 mM HEPES 7.5, and 100 mM NaCl. Crystallization of forms 2 and 3 is described in the [Supplemental Data](#). Crystals were cryoprotected with 20% 2-methyl-2,4-pentanediol or 20% glycerol before mounting in loops and flash freezing in liquid nitrogen. Diffraction data were collected at Beamline 8.3.1 at the Advanced Light Source ([MacDowell et al., 2004](#)). The structure of Aa-ZBD/RPD was solved to 2.0 Å resolution (form 1) by a combination of multiwavelength anomalous dispersion (MAD) phasing from a thulium-chloride-soaked crystal and molecular replacement into high-resolution native data ([Supplemental Data](#)).

E. coli DnaG ZBD and ZBD/RPD Cloning and Labeling

QuikChange (Stratagene) was used to generate the Thr348Cys mutation in the Ec-ZBD/RPD. Constructs were purified by using the procedure outlined above, except that the gel filtration buffer excluded 2-mercaptoethanol. Purified proteins were labeled with fluorophores by incubating with 10-fold molar excess of fluorescein-5-maleimide, tetramethylrhodamine-6-maleimide, or both (Molecular Probes). Labeling reactions were stopped by addition of 5 mM 2-mercaptoethanol, and excess dye was removed with an S-200 gel filtration column (75 mM potassium glutamate, 20 mM HEPES 7.5, 10% glycerol, and 5 mM 2-mercaptoethanol). After spectrophotometric quantification ensured equal labeling efficiencies of the two dyes, peak fractions were snap frozen and stored at –80°C.

SAXS of the *E. coli* ZBD/RPD

Experimental X-ray scattering data were collected at the SIBYLS Beamline 12.3.1 of the Advanced Light Source (Lawrence Berkeley National Laboratory) on Ec-ZBD/RPD dialyzed into buffer B (20 mM HEPES [pH 7.5]; 75 mM potassium glutamate) and serially diluted to 15 mg/ml, 7.5 mg/ml, and 3 mg/ml. Scattering data also were collected on protein dialyzed into buffer B plus 150 mM MgCl₂ or 300 mM MgCl₂. Scattering patterns were recorded at a sample-detector distance of 1.45 m, wavelength of 1.293 Å, and exposures ranging from 1 to 120 s, depending on protein concentration. A composite curve was generated from the various protein concentrations and exposures by using PRIMUS ([Konarev et al., 2003](#)) and evaluated by using GNOM ([Svergun, 1992](#)). Ten independent dummy-residue domain models were built by using CREDO ([Svergun et al., 2001](#)), supplied with the known structure of the *E. coli* RPD (PDB code 1DDE) and the experimental scattering data. All ten models showed an elongated structure that packs against the N terminus of the polymerase domain ([Figure 2A](#)). Although seven models were in excellent agreement with each other as defined by their normalized spatial discrepancy (NSD = 0.520–0.619), three models did not align well with either each other or with the other seven (NSD > 1.0) and were inconsistent with the known structure of the ZBD. These models were discarded as outliers for all subsequent analyses, as is common practice ([Volkov and Svergun, 2003](#)). SUPCOMB and the DAMAVER suite ([Volkov and Svergun, 2003](#)) were used to generate an averaged most-populated-volume envelope from the seven remaining models, into which a threaded structure of the *E. coli* ZBD (based on the *B. stearothermophilus* ZBD structure; [[Pan and Wigley, 2000](#)]), was manually docked. CRY SOL ([Svergun et al.,](#)

1995) was used to generate theoretical scattering curves where applicable.

FRET Measurements of the *E. coli* ZBD/RPD Interaction

FRET measurements were made on a PerkinElmer Victor³V plate reader by using the following filters: ex 485 nm, 14 nm bandpass; em 520 nm, 10 nm bandpass; ex 531 nm, 25 nm bandpass; and em 580 nm, 15 nm bandpass. Reactions were performed in triplicate in 20 mM HEPES (pH 7.5), 0.1 mg/ml BSA, 2 mM DTT, 50 mM K⁺ glutamate, and 50 nM of the labeled molecule. For heteroduplex substrates, RNA (Dharmacon) was annealed to DNA (MWG Biotech) by using a thermal cycler (RNA 5'-GCGGCGGCA-3', DNA 5'-AAAAGTCCGCCGC-3'). Measurements of single-stranded DNA alone were made by using the same oligonucleotide present in the RNA/DNA hybrid. Nucleic acids were present at 100 μM in the reaction. Reactions were allowed to equilibrate at room temperature for 30 min before measurement. FRET efficiencies were calculated by using the method of [Gordon et al. \(1998\)](#).

Primer Synthesis Assay

Asp269Ala and Asp347Ala mutations were introduced into the *E. coli* RPD by QuikChange. Each reaction contained 100 mM potassium glutamate; 50 mM HEPES (pH 7.5); 5 mM magnesium acetate; 1 mM DTT; 1.2 mM spermidine; 0.1 mM each ATP, GTP, and CTP; 10 μCi [α -³²P] UTP; and 40 nM single-stranded DNA template (MWG Biotech). The assay comparing either purified RPD or ZBD/RPD contained 46 μM protein, whereas the *trans* priming assay contained 34 μM of each construct. Reactions were equilibrated for 30 min at room temperature before addition of rNTPs and incubation at 37°C for 1 hr. Salts and free label were removed by using BioRad P-6 Spin Columns equilibrated with 90% formamide and 10 mM EDTA. Samples were heat denatured, loaded on a prerun 7 M urea/20% polyacrylamide TBE gel, and run in TBE. Gels were directly exposed to a phosphorimager screen for one hour and then evaluated on a Molecular Dynamics Typhoon 8600. The template “+0” was 5'-ACACACACTGCAAAGCCAAAAGGAC-3'. The “+X” templates are longer, where “X” stands for the number of additional A/C bases on the 5' terminus (see [Supplemental Data](#)).

Supplemental Data

Supplemental Data include Supplemental Results, Supplemental Experimental Procedures, and three figures and are available with this article online at <http://www.molecule.org/cgi/content/full/20/3/391/DC1/>.

Acknowledgments

We thank C. Chu, E. Cunningham, J. Keck, S. Lynch, D. Mai, A. Schoeffler, and E. Skordalakes for technical assistance and D. Minor and J. Kuriyan for critically reading the manuscript. We also thank G. Meigs and J. Holton at the Advanced Light Source (Berkeley, CA). This work was supported by the G. Harold and Leily Y. Mathers Foundation and the National Institutes of Health (GM071747). Work by G.L.H. was supported by the National Cancer Institute (CA92584).

Received: May 18, 2005

Revised: August 12, 2005

Accepted: September 6, 2005

Published: November 10, 2005

References

- Aloy, P., Ceulemans, H., Stark, A., and Russell, R.B. (2003). The relationship between sequence and interaction divergence in proteins. *J. Mol. Biol.* 332, 989–998.
- Bernstein, J.A., and Richardson, C.C. (1988). A 7-kDa region of the bacteriophage T7 gene 4 protein is required for primase but not for helicase activity. *Proc. Natl. Acad. Sci. USA* 85, 396–400.
- Bird, L.E., Pan, H., Soutanas, P., and Wigley, D.B. (2000). Mapping protein-protein interactions within a stable complex of DNA primase and DnaB helicase from *Bacillus stearothermophilus*. *Biochemistry* 39, 171–182.

- Brejck, K., van Dijk, W.J., Klaassen, R.V., Schuurmans, M., van Der Oost, J., Smit, A.B., and Sixma, T.K. (2001). Crystal structure of an ACh-binding protein reveals the ligand-binding domain of nicotinic receptors. *Nature* **411**, 269–276.
- DeLano, W.L. (2002). The PyMOL Molecular Graphics System <http://pymol.sourceforge.net>.
- Godson, G.N., Schoenich, J., Sun, W., and Mustaev, A.A. (2000). Identification of the magnesium ion binding site in the catalytic center of *Escherichia coli* primase by iron cleavage. *Biochemistry* **39**, 332–339.
- Gordon, G.W., Berry, G., Liang, X.H., Levine, B., and Herman, B. (1998). Quantitative fluorescence resonance energy transfer measurements using fluorescence microscopy. *Biophys. J.* **74**, 2702–2713.
- Griep, M.A., and Mesman, T.N. (1995). Fluorescent labeling of cysteine 39 on *Escherichia coli* primase places the dye near an active site. *Bioconjug. Chem.* **6**, 673–682.
- Johnson, S.K., Bhattacharyya, S., and Griep, M.A. (2000). DnaB helicase stimulates primer synthesis activity on short oligonucleotide templates. *Biochemistry* **39**, 736–744.
- Kato, M., Ito, T., Wagner, G., Richardson, C., and Ellenberger, T. (2003). Modular architecture of the bacteriophage T7 primase couples RNA primer synthesis to DNA synthesis. *Mol. Cell* **11**, 1349–1360.
- Kato, M., Ito, T., Wagner, G., and Ellenberger, T. (2004). A molecular handoff between bacteriophage T7 DNA primase and T7 DNA polymerase Initiates DNA synthesis. *J. Biol. Chem.* **279**, 30554–30562.
- Keck, J., Roche, D., Lynch, S., and Berger, J. (2000). Structure of the RNA polymerase domain of *E. coli* primase. *Science* **287**, 2482–2486.
- Khopde, S., Biswas, E.E., and Biswas, S.B. (2002). Affinity and sequence specificity of DNA binding and site selection for primer synthesis by *Escherichia coli* primase. *Biochemistry* **41**, 14820–14830.
- Kitani, T., Yoda, K., Ogawa, T., and Okazaki, T. (1985). Evidence that discontinuous DNA replication in *Escherichia coli* is primed by approximately 10 to 12 residues of RNA starting with a purine. *J. Mol. Biol.* **184**, 45–52.
- Konarev, P.V., Volkov, V.V., Sokolova, A.V., Koch, M.H.J., and Svergun, D.I. (2003). PRIMUS: a Windows PC-based system for small-angle scattering data analysis. *J. Appl. Crystallogr.* **36**, 1277–1282.
- Kornberg, A., and Baker, T. (1992). *DNA Replication*, Second Edition (New York: Freeman).
- Kusakabe, T., Hine, A.V., Hyberts, S.G., and Richardson, C.C. (1999). The Cys4 zinc finger of bacteriophage T7 primase in sequence-specific single-stranded DNA recognition. *Proc. Natl. Acad. Sci. USA* **96**, 4295–4300.
- Lee, S.J., and Richardson, C.C. (2002). Interaction of adjacent primase domains within the hexameric gene 4 helicase-primase of bacteriophage T7. *Proc. Natl. Acad. Sci. USA* **99**, 12703–12708.
- Lewin, B. (1987). *Genes*, Third Edition (New York: John Wiley & Sons).
- MacDowell, A.A., Celestre, R.S., Howells, M., McKinney, W., Krupnick, J., Cambie, D., Domning, E.E., Duarte, R.M., Kelez, N., Plate, D.W., et al. (2004). Suite of three protein crystallography beamlines with single superconducting bend magnet as the source. *J. Synchrotron Radiat.* **11**, 447–455.
- Mendelman, L.V., Beauchamp, B.B., and Richardson, C.C. (1994). Requirement for a zinc motif for template recognition by the bacteriophage T7 primase. *EMBO J.* **13**, 3909–3916.
- Mitkova, A.V., Khopde, S.M., and Biswas, S.B. (2003). Mechanism and stoichiometry of interaction of DnaG primase with DnaB helicase of *Escherichia coli* in RNA primer synthesis. *J. Biol. Chem.* **278**, 52253–52261.
- Norcum, M.T., Warrington, J.A., Spiering, M.M., Ishmael, F.T., Trakselis, M.A., and Benkovic, S.J. (2005). Architecture of the bacteriophage T4 primosome: electron microscopy studies of helicase (gp41) and primase (gp61). *Proc. Natl. Acad. Sci. USA* **102**, 3623–3626.
- Oakley, A.J., Loscha, K.V., Schaeffer, P.M., Liepinsh, E., Pintacuda, G., Wilce, M.C., Otting, G., and Dixon, N.E. (2005). Crystal and solution structures of the helicase-binding domain of *Escherichia coli* primase. *J. Biol. Chem.* **280**, 11495–11504.
- Okazaki, R., Okazaki, T., Sakabe, K., Sugimoto, K., and Sugino, A. (1968). Mechanism of DNA chain growth. I. Possible discontinuity and unusual secondary structure of newly synthesized chains. *Proc. Natl. Acad. Sci. USA* **59**, 598–605.
- Pan, H., and Wigley, D. (2000). Structure of the zinc-binding domain of *Bacillus stearothermophilus* DNA primase. *Structure* **8**, 231–239.
- Park, S.Y., Beel, B.D., Simon, M.I., Bilwes, A.M., and Crane, B.R. (2004). In different organisms, the mode of interaction between two signaling proteins is not necessarily conserved. *Proc. Natl. Acad. Sci. USA* **101**, 11646–11651.
- Podobnik, M., McInerney, P., O'Donnell, M., and Kuriyan, J. (2000). A TOPRIM domain in the crystal structure of the catalytic core of *Escherichia coli* primase confirms a structural link to DNA topoisomerases. *J. Mol. Biol.* **300**, 353–362.
- Richey, B., Cayley, D.S., Mossing, M.C., Kolka, C., Anderson, C.F., Farrar, T.C., and Record, M.T., Jr. (1987). Variability of the intracellular ionic environment of *Escherichia coli*. Differences between in vitro and in vivo effects of ion concentrations on protein-DNA interactions and gene expression. *J. Biol. Chem.* **262**, 7157–7164.
- Shrimankar, P., Stordal, L., and Maurer, R. (1992). Purification and characterization of a mutant DnaB protein specifically defective in ATP hydrolysis. *J. Bacteriol.* **174**, 7689–7696.
- Svergun, D.I. (1992). Determination of the regularization parameter in indirect-transform methods using perceptual criteria. *J. Appl. Crystallogr.* **25**, 495–503.
- Svergun, D.I., Barberato, C., and Koch, M.H. (1995). CRY SOL—a program to evaluate X-ray solution scattering of biological macromolecules from atomic coordinates. *J. Appl. Crystallogr.* **28**, 768–773.
- Svergun, D.I., Petoukhov, M.V., and Koch, M.H. (2001). Determination of domain structure of proteins from X-ray solution scattering. *Biophys. J.* **80**, 2946–2953.
- Swart, J.R., and Griep, M.A. (1995). Primer synthesis kinetics by *Escherichia coli* primase on single-stranded DNA templates. *Biochemistry* **34**, 16097–16106.
- Syson, K., Thirlway, J., Hounslow, A.M., Soutanas, P., and Waltho, J.P. (2005). Solution structure of the helicase-interaction domain of the primase DnaG: a model for helicase activation. *Structure* **13**, 609–616.
- Toth, E.A., Li, Y., Sawaya, M.R., Cheng, Y., and Ellenberger, T. (2003). The crystal structure of the bifunctional primase-helicase of bacteriophage T7. *Mol. Cell* **12**, 1113–1123.
- Tougu, K., and Marians, K. (1996). The interaction between helicase and primase sets the replication fork clock. *J. Biol. Chem.* **271**, 21398–21405.
- Urlacher, T.M., and Griep, M.A. (1995). Magnesium acetate induces a conformational change in *Escherichia coli* primase. *Biochemistry* **34**, 16708–16714.
- Valentine, A.M., Ishmael, F.T., Shier, V.K., and Benkovic, S.J. (2001). A zinc ribbon protein in DNA replication: primer synthesis and macromolecular interactions by the bacteriophage T4 primase. *Biochemistry* **40**, 15074–15085.
- Volkov, V.V., and Svergun, D.I. (2003). Uniqueness of ab initio shape determination in small-angle scattering. *J. Appl. Crystallogr.* **36**, 860–864.
- Wu, C.A., Zechner, E.L., Reems, J.A., McHenry, C.S., and Marians, K.J. (1992). Coordinated leading- and lagging-strand synthesis at the *Escherichia coli* DNA replication fork. V. Primase action regulates the cycle of Okazaki fragment synthesis. *J. Biol. Chem.* **267**, 4074–4083.
- Yang, J., Xi, J., Zhuang, Z., and Benkovic, S.J. (2005). The oligomeric T4 primase is the functional form during replication. *J. Biol. Chem.* **280**, 25416–25423.
- Yang, S., Yu, X., VanLoock, M.S., Jezewska, M.J., Bujalowski, W., and Egelman, E.H. (2002). Flexibility of the rings: structural asymmetry in the DnaB hexameric helicase. *J. Mol. Biol.* **321**, 839–849.

Yuzhakov, A., Kelman, Z., and O'Donell, M. (1999). Trading places on DNA—a three-point switch underlies primer handoff from primase to the replicative DNA polymerase. *Cell* **96**, 153–163.

Zechner, E.L., Wu, C.A., and Marians, K.J. (1992). Coordinated leading- and lagging-strand synthesis at the *Escherichia coli* DNA replication fork. III. A polymerase-primase interaction governs primer size. *J. Biol. Chem.* **267**, 4054–4063.

Accession Numbers

Coordinates have been deposited under accession number [2AU3](#).